

Color superconducting quark matter

Mark Alford

Dept. of Physics and Astronomy, Glasgow University, Glasgow G12 8QQ, UK

KEYWORDS: quark pairing, neutron stars, compact stars, pulsars

ABSTRACT: I review recent progress in our understanding of the color superconducting phase of matter above nuclear density, giving particular emphasis to the effort to find observable signatures of the presence of this phase in compact stars.

CONTENTS

INTRODUCTION	1
<i>The Fermi surface and Cooper instability</i>	2
<i>The gap equation</i>	3
TWO MASSLESS QUARK FLAVORS	6
THREE MASSLESS QUARK FLAVORS	8
TWO MASSLESS + ONE MASSIVE QUARK FLAVORS	11
<i>Description of the phase diagram</i>	12
<i>Quark-hadron continuity</i>	14
COLOR-FLAVOR UNLOCKING AND THE CRYSTALLINE COLOR SUPERCONDUCTING PHASE	17
<i>The (un)locking transition</i>	18
<i>The crystalline color superconducting phase</i>	19
COMPACT STAR PHENOMENOLOGY	22
<i>Cooling by neutrino emission</i>	23
<i>The neutrino pulse at birth</i>	24
<i>r-mode instability</i>	25
<i>Magnetic field decay</i>	26
<i>Glitches and the crystalline color superconductor</i>	27
CONCLUSIONS	29

1 INTRODUCTION

In the last 30 years, the idea that matter has subnuclear constituents (“quarks”) has emerged from the speculative edges of particle physics to become a firmly established physical theory. Quantum Chromodynamics (QCD), the theory of the interaction of quarks via the gluon field, is now one of the pillars of the standard model. In high momentum processes, perturbative QCD has been verified

comprehensively. For the spectrum and structural properties of the hadrons, the strongly-coupled intractability of the theory is giving way to the brute-force numerical methods of lattice QCD, and again yields agreement with experiment. Even so, there remain tantalizing questions. As well as predicting the properties and behavior of small numbers of particles, QCD should also be able to tell us about the thermodynamics of matter in the realm of unimaginably high temperatures and densities at which it comes to dominate the physics. However, only in the last few years have these regions begun to be probed experimentally, and our theoretical understanding of them remains elementary.

Progress has been fastest for matter at high temperature and low density. Lattice gauge calculations (1) show that chiral symmetry is restored and deconfinement occurs at a temperature $T \sim 180$ MeV.

At high densities, in contrast, lattice methods have so far proved unhelpful. We are still trying to establish the symmetries of the ground state, and find effective theories for its lowest excitations. These questions are of direct physical relevance: an understanding of the symmetry properties of dense matter can be expected to inform our understanding of neutron star astrophysics and perhaps also heavy ion collisions which achieve high baryon densities without reaching very high temperatures.

In this review I will explore the progress that has been made in the last few years in understanding the possible phases of QCD at low temperatures and high densities, and go on to discuss the possible observable signatures in compact stars phenomenology. For alternative explanations and emphasis, I refer the reader to previous review articles on this topic (2).

1.1 *The Fermi surface and Cooper instability*

One of the most striking features of QCD is asymptotic freedom: the force between quarks becomes arbitrarily weak as the characteristic momentum scale of their interaction grows larger. This immediately suggests that at sufficiently high densities and low temperatures, matter will consist of a Fermi sea of essentially free quarks, whose behavior is dominated by the freest of them all: the high-momentum quarks that live at the Fermi surface.

Such a picture is too naive. It was shown by Bardeen, Cooper, and Schrieffer (BCS) (3) that in the presence of attractive interactions a Fermi surface is unstable. If there is *any* channel in which the quark-quark interaction is attractive, then the true ground state of the system will not be the naked Fermi surface, but rather a complicated coherent state of particle and hole pairs—“Cooper pairs”.

This can be seen intuitively as follows. Consider a system of free particles. The Helmholtz free energy is $F = E - \mu N$, where E is the total energy of the system, μ is the chemical potential, and N is the number of particles. The Fermi surface is defined by a Fermi energy $E_F = \mu$, at which the free energy is minimized, so adding or subtracting a single particle costs zero free energy. Now, suppose a weak attractive interaction is switched on. BCS showed that this leads to a complete rearrangement of the states near the Fermi surface, because it costs no free energy to make a pair of particles (or holes), and the attractive interaction makes it favorable to do so. Many such pairs will therefore be created, in all

the modes near the Fermi surface, and these pairs, being bosonic, will form a condensate. The ground state will be a superposition of states with all numbers of pairs, breaking the fermion number symmetry. An arbitrarily weak interaction has lead to spontaneous symmetry breaking.

In condensed matter systems, where the relevant fermions are electrons, the necessary attractive interaction has been hard to find. The dominant interaction between electrons is the repulsive electrostatic force, but in the right kind of crystal there are attractive phonon-mediated interactions that can overcome it. In these materials the BCS mechanism leads to superconductivity, since it causes Cooper pairing of electrons, which breaks the electromagnetic gauge symmetry, giving mass to the photon and producing the Meissner effect (exclusion of magnetic fields from a superconducting region). It is a rare and delicate state, easily disrupted by thermal fluctuations, so superconductivity only survives at low temperatures.

In QCD, by contrast, the dominant gauge-boson-mediated interaction between quarks is itself attractive (4,5,6,7,8). The relevant degrees of freedom are those which involve quarks with momenta near the Fermi surface. These interact via gluons, in a manner described by QCD. The quark-quark interaction has two color channels available, the antisymmetric $\bar{\mathbf{3}}$, and the symmetric $\mathbf{6}$. It is attractive in the $\mathbf{3}_A$: this can be seen in single-gluon-exchange or by counting of strings.

Since pairs of quarks cannot be color singlets, the resulting condensate will break the local color symmetry $SU(3)_{\text{color}}$. We call this “color superconductivity”. Note that the quark pairs play the same role here as the Higgs particle does in the standard model: the color-superconducting phase can be thought of as the Higgsed (as opposed to confined) phase of QCD.

It is important to remember that the breaking of a gauge symmetry cannot be characterized by a gauge-invariant local order parameter which vanishes on one side of a phase boundary. The superconducting phase can be characterized rigorously only by its global symmetries. In electromagnetism there is a non-local order parameter, the mass of the magnetic photons, that corresponds physically to the Meissner effect and distinguishes the free phase from the superconducting one. In QCD there is no free phase: even without pairing the gluons are not states in the spectrum. No order parameter distinguishes the Higgsed phase from a confined phase or a plasma, so we have to look at the global symmetries.

In most of this paper we will take an approach similar to that used in analyzing the symmetry breaking of the standard model, and discuss the phases of dense QCD in terms of a gauge-variant observable, the diquark condensate, which is analogous to the vacuum expectation value (VEV) of the Higgs field. However, this is only a convenience, and we will be careful to label different phases by their unbroken global symmetries, so that they can always be distinguished by gauge-invariant order parameters.

1.2 The gap equation

To decide whether or not fermions condense in the ground state, one can explicitly construct a wavefunctional with the appropriate pairing, and use a many-body variational approach. But the field-theoretical approach, though less concrete, is

$$\text{Full propagator} = \text{---} + \text{---} \circlearrowleft \text{---} + \text{---} \circlearrowleft \circlearrowleft \text{---} + \dots$$

$$\text{Self-energy} = \text{---} \circlearrowleft \text{---} + \text{---} \circlearrowleft \circlearrowleft \text{---}$$
Neglect this

Figure 1: Mean-field Schwinger-Dyson (gap) equations

more general, and I will briefly describe it here.

The important quantity is the quark self energy, i.e. the one-particle irreducible (1PI) Green function of two quark fields. Its poles will give the gauge-invariant masses of the quasiquarks, the lowest energy fermionic excitations around the quark Fermi surface. To see if condensation (chiral condensation, flavor-singlet quark pairing, or whatever) occurs in some channel, one writes down a self-consistency equation, the “gap equation”, for a self energy with that structure, and solves it to find the actual self energy (the gap). If it is zero, there is no condensation in that channel. If not, there can be condensation, but it may just be a local minimum of the free energy. There may be other solutions to the gap equation, and the one with the lowest free energy is the true ground state.

There are several possible choices for the interaction to be used in the gap equation. At asymptotically high densities QCD is weakly coupled, so one gluon exchange is appropriate. Such calculations (9, 10, 11, 12, 13, 14, 15, 16, 17, 18) are extremely important, since they demonstrate from first principles that color superconductivity occurs in QCD. However, the density regime of physical interest for neutron stars or heavy ion collisions is up to a few times nuclear density ($\mu \lesssim 500$ MeV) and weak coupling calculations are unlikely to be trustworthy in that regime. In fact, current weak-coupling calculations cannot be extrapolated below about 10^8 MeV because of gauge dependence arising from the neglect of vertex corrections (19). There have also been some preliminary investigations of confinement-related physics such as a gluon condensate (20, 21).

The alternative is to use some phenomenological interaction that can be argued to capture the essential physics of QCD in the regime of interest. The interaction can be normalized to reproduce known low-density physics such as the chiral condensate, and then extrapolated to the desired chemical potential. In two-flavor theories, the instanton vertex is a natural choice (7, 8, 22, 23), since it is a four-fermion interaction. With more flavors, the one gluon exchange vertex without a gluon propagator (6, 24, 25) is more convenient. It has been found that these both give the same results, to within a factor of about 2. This is well within the inherent uncertainties of such phenomenological approaches. In the rest of this paper we will therefore not always be specific about the exact

interaction used to obtain a given result. One caveat to bear in mind is that the single-gluon-exchange interaction is symmetric under $U(1)_A$, and so it sees no distinction between condensates of the form $\langle qCq \rangle$ and $\langle qC\gamma_5q \rangle$. However, once instantons are included the Lorentz scalar $\langle qC\gamma_5q \rangle$ is favored, (7, 8) so in single-gluon-exchange calculations the parity-violating condensate is usually ignored.

The mean-field approximation to the Schwinger-Dyson equations is shown diagrammatically in Figure 1, relating the full propagator to the self-energy. In the mean-field approximation, only daisy-type diagrams are included in the resummation, vertex corrections are excluded. Algebraically, the equation takes the form

$$\Sigma(k) = -\frac{1}{(2\pi)^4} \int d^4q M^{-1}(q)D(k-q), \quad (1)$$

where $\Sigma(k)$ is the self-energy, M is the full fermion matrix (inverse full propagator), and $D(k-q)$ is the vertex, which in NJL models will be momentum-independent, but in a weak-coupling QCD calculation will include the gluon propagator and couplings. Since we want to study quark-quark condensation, we have to write propagators in a form that allows for this possibility, just as to study chiral symmetry breaking it is necessary to use 4-component Dirac spinors rather than 2-component Weyl spinors, even if there is no mass term in the action. We therefore use Nambu-Gorkov 8-component spinors, $\Psi = (\psi, \bar{\psi}^T)$, so the self-energy Σ can include a quark-quark pairing term Δ . The fermion matrix M then takes the form

$$M(q) = M_{\text{free}} + \Sigma = \begin{pmatrix} \not{q} + \mu\gamma_0 & \gamma_0\Delta\gamma_0 \\ \Delta & (\not{q} - \mu\gamma_0)^T \end{pmatrix}. \quad (2)$$

Equations (1) and (2) can be combined to give a self-consistency condition for Δ , the gap equation. If the interaction is a point-like four-fermion NJL interaction then the gap parameter Δ will be a color-flavor-spin matrix, independent of momentum. If the gluon propagator is included, Δ will be momentum-dependent, complicating the analysis considerably.

In NJL models, the simplicity of the model has allowed renormalization group analyses (26, 27) that include a large class of four-fermion interactions, and follow their running couplings as modes are integrated out. This confirms that in QCD with two and three massless quarks the most attractive channels for condensation are those corresponding to the ‘‘2SC’’ and ‘‘CFL’’ phases studied below. Calculations using random matrices, which represent very generic systems, also show that diquark condensation is favored at high density (28).

Following through the analysis outlined above, one typically finds gap equations of the form

$$1 = K \int_0^\Lambda k^2 dk \frac{1}{\sqrt{(k-\mu)^2 + \Delta^2}}, \quad (3)$$

where K is the NJL four-fermion coupling. In the limit of small gap, the integral can be evaluated, giving

$$\Delta \sim \Lambda \exp\left(\frac{\text{const}}{K\mu^2}\right). \quad (4)$$

This shows the non-analytic dependence of the gap on the coupling K . Condensation is a nonperturbative effect that cannot be seen to any order in perturbation theory. The reason it can be seen in the diagrammatic Schwinger-Dyson approach is that there is an additional ingredient: an ansatz for the form of the self energy. This corresponds to guessing the form of the ground state wavefunction in a many-body variational approach. All solutions to gap equations therefore represent possible stable ground states, but to find the favored ground state their free energies must be compared, and even then one can never be sure that the true ground state has been found, since there is always the possibility that there is another vacuum that solves its own gap equation and has an even lower free energy.

In weak-coupling QCD calculations, where the full single-gluon-exchange vertex complete with gluon propagator is used, the gap equation takes the form (4, 5, 9, 13)

$$\Delta \sim \mu \frac{1}{g^5} \exp\left(-\frac{3\pi^2}{\sqrt{2}} \frac{1}{g}\right), \quad (5)$$

or, making the weak-coupling expansion in the QCD gauge coupling g more explicit,

$$\ln\left(\frac{\Delta}{\mu}\right) = -\frac{3\pi^2}{\sqrt{2}} \frac{1}{g} - 5 \ln g + \text{const} + \mathcal{O}(g). \quad (6)$$

This gap equation has two interesting features. Firstly, it does not correspond to what you would naively expect from the NJL model of single gluon exchange, in which the gluon propagator is discarded and $K \propto g^2$, yielding $\Delta \sim \exp(-1/g^2)$. The reason (5, 9) is that at high density the gluon propagator has an infrared divergence at very small angle scattering, since magnetic gluons are only Landau damped, not screened. This divergence is regulated by the gap itself, weakening its dependence on the coupling.

Secondly, in (5) we have left unspecified the energy scale at which the coupling g is to be evaluated. Natural guesses would be μ or Δ . If we use $g(\mu)$ and assume it runs according to the one-loop formula $1/g^2 \sim \ln \mu$ then the exponential factor in (5) gives very weak suppression, and is in fact overwhelmed by the initial factor μ , so that the gap rises without limit at asymptotically high density, although Δ/μ shrinks to zero so that weak-coupling methods are still self-consistent. This means that color superconductivity will inevitably dominate the physics at high enough densities.

2 TWO MASSLESS QUARK FLAVORS

In the real world there are two light quark flavors, the up (u) and down (d), with masses $\lesssim 10$ MeV, and a medium-weight flavor, the strange (s) quark, with mass ~ 100 MeV. A first approximation is to ignore the strange, and set $m_{u,d} = 0$.

The gap equation for this scenario has been solved using various interactions: pointlike four-fermion interactions based on the instanton vertex (4, 7, 8, 22), a full instanton vertex including all the form factors (23), and a weakly coupled gluon propagator (10, 13, 11, 14, 15, 16). All agree that the quarks prefer to pair

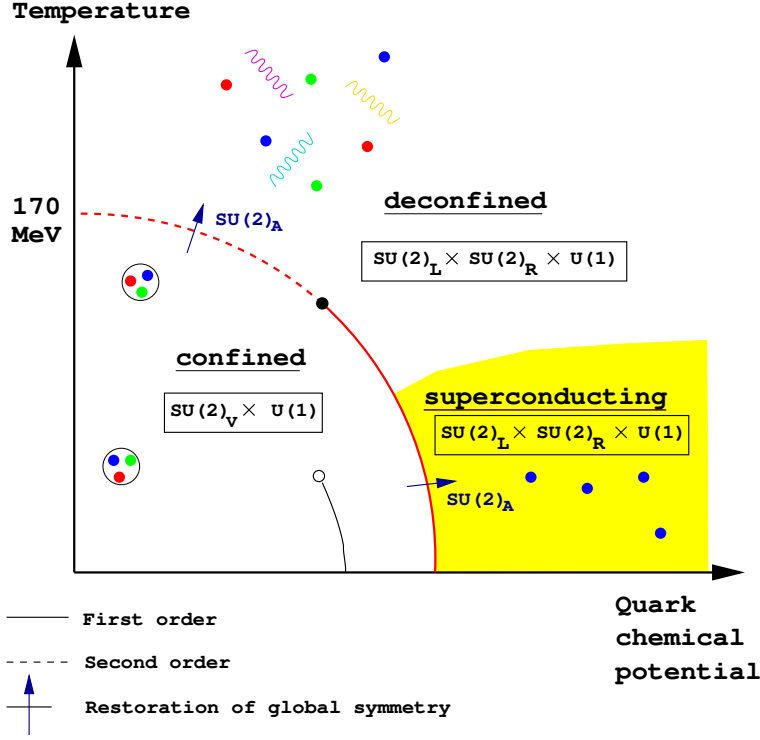


Figure 2: Two massless flavor phase diagram

in the color $\bar{\mathbf{3}}$ flavor singlet channel

$$2\text{SC phase: } \Delta_{ij}^{\alpha\beta} = \langle q_i^\alpha q_j^\beta \rangle_{1PI} \propto C \gamma_5 \epsilon_{ij} \epsilon^{\alpha\beta 3} \quad (7)$$

(color indices α, β run from 1 to 3, flavor indices i, j run from 1 to 2). The four-fermion interaction calculations also agree on the magnitude of Δ : around 100 MeV. This is found to be roughly independent of the cutoff, although the chemical potential at which it is attained is not. Such calculations are based on calibrating the coupling to give a chiral condensate of around 400 MeV at zero density, and turning μ up to look for the maximum gap.

As with any spontaneous symmetry breaking, one of the degenerate ground states is arbitrarily selected. In this case, quarks of the first two colors (red and green) participate in pairing, while the third color (blue) does not. The ground state is invariant under an $SU(2)$ subgroup of the color rotations that mixes red and green, but the blue quarks are singled out as different. The pattern of symmetry breaking is therefore (with gauge symmetries in square brackets)

$$\begin{aligned} & [SU(3)_{\text{color}}] \times [U(1)_Q] \times SU(2)_L \times SU(2)_R \\ \longrightarrow & [SU(2)_{\text{color}}] \times [U(1)_{\tilde{Q}}] \times SU(2)_L \times SU(2)_R \end{aligned} \quad (8)$$

The expected phase diagram in the μ - T plane is shown in Figure 2. The features of this pattern of condensation are

- The color gauge group is broken down to $SU(2)$, so five of the gluons will become massive, with masses of order the gap (since the coupling is of

order 1). The remaining three gluons are associated with an unbroken $SU(2)$ red-green gauge symmetry, whose confinement distance scale rises exponentially with density (29).

- The red and green quark modes acquire a gap Δ , which is the mass of the physical excitations around the Fermi surface (quasiquarks). There is no gap for the blue quarks in this ansatz, and it is an interesting question whether they find some other channel in which to pair. The available attractive channels appear to be weak so the gap will be much smaller, perhaps in the keV range (7, 30). It has even been suggested that 'tHooft anomaly matching may prevent any condensation (31, 32).
- Electromagnetism is broken, but this does not mean that the 2SC phase is an electromagnetic as well as a color superconductor. Just as in the standard model the Higgs VEV leaves unbroken a linear combination Q of the weak W_3 and hypercharge Y bosons, so here a linear combination \tilde{Q} of the eighth gluon T_8 and the electric charge Q is left unbroken. This plays the role of a “rotated” electromagnetism. We will discuss some of its physical effects in a later section.
- No global symmetries are broken (although additional condensates that break chirality have been suggested (33)) so the 2SC phase has the same symmetries as the quark-gluon plasma (QGP), so there need not be any phase transition between them. Again, this is in close analogy to the physics of the standard model, where the Higgs VEV breaks no global symmetries: the phase transition line between the unbroken and broken phases ends at some critical Higgs mass, and the two regimes are analytically connected. The reader may wonder why one cannot construct an order parameter to distinguish the 2SC phase using the fact that the quark pair condensate blatantly breaks baryon number, which is a global symmetry. However, in the two flavor case baryon number is a linear combination of electric charge and isospin, $B = 2Q - 2I_3$, so baryon number is already included in the symmetry groups of Eq. (8). Just as an admixture of gluon and photon survives unbroken as a rotated electromagnetism, so an admixture of B and T_8 survives unbroken as a rotated baryon number.

3 THREE MASSLESS QUARK FLAVORS

In QCD with three flavors of massless quarks the Cooper pairs *cannot* be flavor singlets, and both color and flavor symmetries are necessarily broken (25) (see also (34) for zero density). The gap equation has been solved for pointlike 4-fermion interactions with the index structure of single gluon exchange (25, 35, 36) as well as a weakly coupled gluon propagator (17, 18). They agree that the attractive channel exhibits a pattern called color-flavor locking (CFL),

$$\begin{aligned} \text{CFL phase: } \Delta_{ij}^{\alpha\beta} = \langle q_i^\alpha q_j^\beta \rangle_{1PI} &\propto C\gamma_5[\varepsilon^{\alpha\beta X} \varepsilon_{ijX} + \kappa(\delta_i^\alpha \delta_j^\beta + \delta_j^\alpha \delta_i^\beta)] \\ &\propto C\gamma_5[(\kappa + 1)\delta_i^\alpha \delta_j^\beta + (\kappa - 1)\delta_j^\alpha \delta_i^\beta] \end{aligned} \quad (9)$$

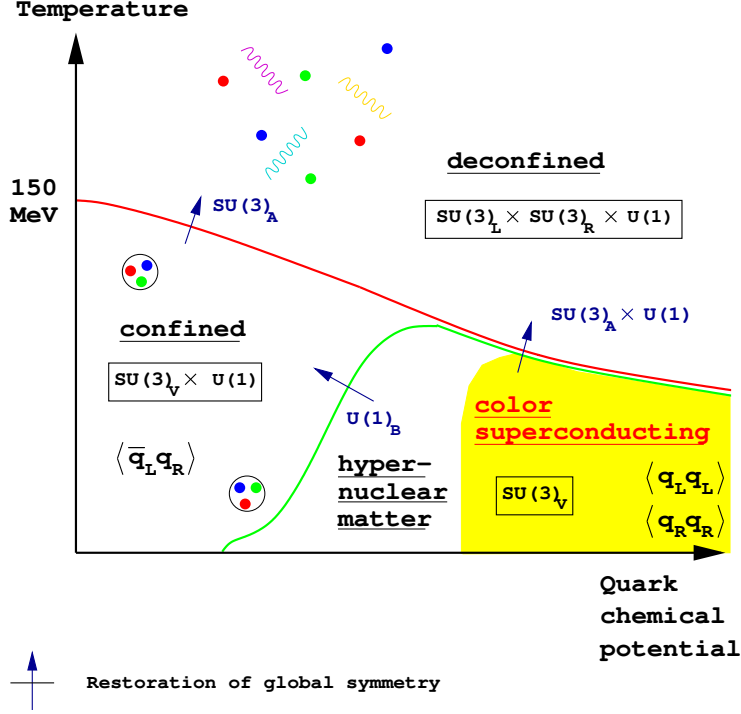


Figure 3: Three massless flavor phase diagram

(color indices α, β and flavor indices i, j all run from 1 to 3). The first line shows the connection between this and the 2SC pairing pattern. When $\kappa = 0$ the pairing is in the $(\bar{\mathbf{3}}_A, \bar{\mathbf{3}}_A)$ channel of color and flavor, which corresponds to three orthogonal copies of the 2SC pairing: the red and green u and d pair as in 2SC, in addition the red and blue u and s pair, and finally the green and blue d and s pair. The term multiplied by κ corresponds to pairing in the $(\mathbf{6}_S, \mathbf{6}_S)$. It turns out that this additional condensate, although not highly favored energetically (the color $\mathbf{6}_S$ is not attractive in single gluon exchange, instanton vertex, or strong coupling) breaks no additional symmetries and so κ is in general small but not zero (25,37). A weak-coupling calculation (17) shows that κ is suppressed by one power of the coupling, $\kappa = g\sqrt{2}\log(2)/(36\pi)$.

The second line of Eq. (9) exhibits the color-flavor locking property of this ground state. The Kronecker deltas dot color indices with flavor indices, so that the VEV is not invariant under color rotations, nor under flavor rotations, but only under simultaneous, equal and opposite, color and flavor rotations. Since color is only a vector symmetry, this VEV is only invariant under vector flavor rotations, and breaks chiral symmetry.

The pattern of symmetry breaking is therefore

$$[SU(3)_{\text{color}}] \times \underbrace{SU(3)_L \times SU(3)_R}_{\supset [U(1)_Q]} \times U(1)_B \longrightarrow \underbrace{SU(3)_{C+L+R}}_{\supset [U(1)_{\bar{Q}}]} \times \mathbb{Z}_2 \quad (10)$$

The expected phase diagram in the μ - T plane is shown in Figure 3. The features of this pattern of condensation are

- The color gauge group is completely broken. All eight gluons become massive. This ensures that there are no infrared divergences associated with gluon propagators.
- All the quark modes are gapped. The nine quasi-quarks (three colors times three flavors) fall into an $\mathbf{8} \oplus \mathbf{1}$ of the unbroken global $SU(3)$, so there are two gap parameters. The singlet has a larger gap than the octet.
- Electromagnetism is no longer a separate symmetry, but corresponds to gauging one of the flavor generators. A rotated electromagnetism (“ \tilde{Q} ”) survives unbroken. Just as in the 2SC case it is a combination of the original photon and one of the gluons, although the relative coefficients are different.
- Two global symmetries are broken, the chiral symmetry and baryon number, so there are two gauge-invariant order parameters that distinguish the CFL phase from the QGP, and corresponding Goldstone bosons which are long-wavelength disturbances of the order parameter. The order parameter for the chiral symmetry is $\langle \bar{\psi}_L \gamma_\mu \lambda^A \psi_L \bar{\psi}_R \gamma_\mu \lambda^A \psi_R \rangle$ where λ^A are the flavor generators (17) (which only gets a vacuum expectation value beyond the mean field approximation). The chiral Goldstone bosons form a pseudoscalar octet, like the zero-density $SU(3)_{\text{flavor}}$ pion octet. The breaking of the baryon number symmetry has order parameter $\langle udsuds \rangle = \langle \Lambda \Lambda \rangle$, and a singlet scalar Goldstone boson which makes the CFL phase a superfluid. If a quark mass were introduced then it would explicitly break the chiral symmetry and give a mass to the chiral Goldstone octet, but the CFL phase would still be a superfluid, distinguished by its baryon number breaking.
- Quark-hadron continuity. It is striking that the symmetries of the 3-flavor CFL phase are the same as those one might expect for 3-flavor hypernuclear matter (35). In hypernuclear matter one would expect the hyperons to pair in an $SU(3)_{\text{flavor}}$ singlet ($\langle \Lambda \Lambda \rangle, \langle \Sigma \Sigma \rangle, \langle N \Xi \rangle$), breaking baryon number but leaving flavor and electromagnetism unbroken. Chiral symmetry would be broken by the chiral condensate. This means that one might be able to follow the spectrum continuously from hypernuclear matter to the CFL phase of quark matter—there need be no phase transition. The pions would evolve into the pseudoscalar octet mentioned above. The vector mesons would evolve into the massive gauge bosons. This will be discussed in more detail below for the 2+1 flavor case.

We can now draw a hypothetical phase diagram for 3-flavor QCD (Figure 3). Comparing with the 2-flavor case, we see that the 2SC quark-paired phase is easy to distinguish from nuclear matter, since it has restored chiral symmetry, but hard to distinguish from the QGP. The CFL phase is easy to distinguish from the QGP, but hard to distinguish from hypernuclear matter.

We conclude that dense quark matter has rather different global symmetries for $m_s = 0$ than for $m_s = \infty$. Since the real world has a strange quark of middling mass, it is very interesting to see what happens as one interpolates between these extremes.

Table 1: Symmetries of phases of QCD.

phase	electromagnetism	chiral symmetry	baryon number
QGP	Q	unbroken	B
2 flavor nuclear matter	broken	broken	broken
2 flavor quark pairing (2SC)	$\tilde{Q} = Q - \frac{1}{2\sqrt{3}}T_8$	unbroken	$\tilde{B} = \tilde{Q} + I_3$
3 flavor nuclear matter	Q	broken	broken
3 flavor quark pairing (CFL)	$\tilde{Q} = Q + \frac{1}{\sqrt{3}}T_8$	broken	broken

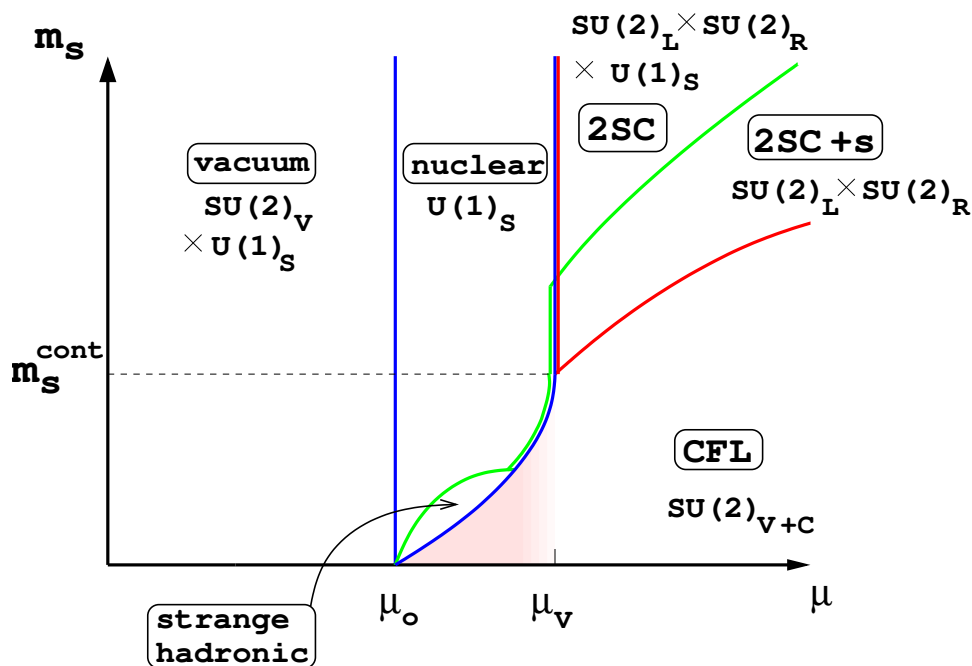


Figure 4: Conjectured phase diagram for 2+1 flavor QCD at $T = 0$. The global symmetries of each phase are labelled. The red line marks chiral symmetry breaking, the blue line isospin breaking, and the green line strangeness breaking. The regions of the phase diagram labelled 2SC, 2SC+s and CFL denote color superconducting quark matter phases. The pink shading marks the region of quark-hadron continuity. A detailed explanation is given in the text.

4 TWO MASSLESS + ONE MASSIVE QUARK FLAVORS

A nonzero strange quark mass explicitly breaks the flavor $SU(3)_L \times SU(3)_R$ symmetry down to $SU(2)_L \times SU(2)_R$. If the strange quark is heavy enough then it will decouple, and 2SC pairing will occur. For a sufficiently small strange quark mass we expect a reduced form of color-flavor locking in which an $SU(2)$ subgroup of $SU(3)_{\text{color}}$ locks to isospin, causing chiral symmetry breaking and

leaving a global $SU(2)_{\text{color}+V}$ group unbroken.

As m_s is increased from zero to infinity, there has to be some critical value at which the strange quark decouples, color and flavor rotations are unlocked, and the full $SU(2)_L \times SU(2)_R$ symmetry is restored. It can be argued on general grounds (see below) that a simple unlocking phase transition must be first order, although there are strong indications that there is a crystalline intermediate phase (see Section 5).

An analysis of the unlocking transition, using a NJL model with interaction based on single-gluon exchange (38, 35) confirms this expectation. Although the quantitative results from NJL models can only be regarded as rough approximations, it is interesting that the calculations indicate that for realistic values of the strange quark mass chiral symmetry breaking may be present for densities all the way down to those characteristic of baryonic matter. This raises the possibility that quark matter and baryonic matter may be continuously connected in nature, as Schäfer and Wilczek have conjectured for QCD with three massless quarks (35). The gaps due to pairing at the quark Fermi surfaces map onto gaps due to pairing at the baryon Fermi surfaces in superfluid baryonic matter consisting of nucleons, Λ 's, Σ 's, and Ξ 's (see below).

Based on the NJL calculations, the zero-temperature phase diagram as a function of chemical potential and strange quark mass has been conjectured (38) to be as shown in Figure 4. Electromagnetism was ignored in this calculation, and it was assumed that wherever a baryon Fermi surface is present, baryons always pair at zero temperature. To simplify our analysis, we assume that baryons always pair in channels which preserve rotational invariance, breaking internal symmetries such as isospin if necessary. So the real phase diagram may well be even more complicated.

We characterize the phases using the $SU(2)_L \times SU(2)_R$ flavor rotations of the light quarks, and the $U(1)_S$ rotations of the strange quarks. The $U(1)_B$ symmetry associated with baryon number is a combination of $U(1)_S$, a $U(1)$ subgroup of isospin, and the gauged $U(1)_{\text{EM}}$ of electromagnetism. Therefore, in our analysis of the global symmetries, once we have analyzed isospin and strangeness, considering baryon number adds nothing new.

4.1 Description of the phase diagram

To explain Figure 4, we follow the phases that occur from low to high density, first for large m_s , then small m_s .

4.1.1 Heavy strange quark

For $\mu = 0$ the density is zero; isospin and strangeness are unbroken; Lorentz symmetry is unbroken; chiral symmetry is broken. Above a first order transition (39) at an onset chemical potential $\mu_o \sim 300$ MeV, one finds nuclear matter. Lorentz symmetry is broken, leaving only rotational symmetry manifest. Chiral symmetry is broken, though perhaps with a reduced chiral condensate. We expect an instability of the nucleon Fermi surfaces to lead to Cooper pairing, and assume that, as is observed in nuclei, the pairing is pp and nn , breaking isospin (and

perhaps also rotational invariance). Since there are no strange baryons present, $U(1)_S$ is unbroken. When μ is increased above μ_V , we find the “2SC” phase of color-superconducting matter consisting of up and down quarks only, paired in Lorentz singlet isosinglet channels. The full flavor symmetry $SU(2)_L \times SU(2)_R$ is restored. The phase transition at μ_V is first order according to NJL models with low cutoff (22, 40, 41, 23) and random matrix models (42) as the chiral condensate competes with the superconducting condensate.

When μ exceeds the constituent strange quark mass $M_s(\mu)$, a strange quark Fermi surface forms, with a Fermi momentum far below that for the light quarks. The strange quarks pair with each other, in a color-spin locked phase (43) that we call “2SC+s”. Strangeness is now broken, but the ss condensate is expected to be small (43).

Finally, when the chemical potential is high enough that the Fermi momenta for the strange and light quarks become comparable, we cross into the color-flavor locked (CFL) phase. There is an unbroken global symmetry constructed by locking the $SU(2)_V$ isospin rotations and an $SU(2)$ subgroup of color. Chiral symmetry is once again broken.

4.1.2 Light strange quark

Below μ_o , we have the vacuum, as before. At μ_o , one enters the nuclear matter phase, with the familiar nn and pp pairing at the neutron and proton Fermi surfaces breaking isospin.

At a somewhat larger chemical potential, strangeness is broken, first perhaps by kaon condensation (44, 45, 46) or by the appearance and Cooper pairing of strange baryons, Λ and Σ , and then Ξ , which pair with themselves in spin singlets. This phase is labelled “strange hadronic” in Figure 4. The global symmetries $SU(2)_L \times SU(2)_R$ and $U(1)_S$ are all broken.

We can imagine two possibilities for what happens next as μ increases further, and we enter the pink region of the figure. (1) Deconfinement: the baryonic Fermi surface is replaced by u, d, s quark Fermi surfaces, which are unstable against pairing, and we enter the CFL phase, described above. Isospin is locked to color and $SU(2)_{\text{color}+V}$ is restored, but chiral symmetry remains broken. (2) No deconfinement: the Fermi momenta of all of the octet baryons are now similar enough that pairing between baryons with differing strangeness becomes possible. At this point, isospin is restored: the baryons pair in rotationally invariant isosinglets ($p\Xi^-$, $n\Xi^0$, $\Sigma^+\Sigma^-$, $\Sigma^0\Sigma^0$, $\Lambda\Lambda$). The interesting point is that scenario (1) and scenario (2) are indistinguishable. Both look like the “CFL” phase of the figure: $U(1)_S$ and chirality are broken, and there is an unbroken vector $SU(2)$. This is the “continuity of quark and hadron matter” described by Schäfer and Wilczek (35). We conclude that for low enough strange quark mass, $m_s < m_s^{\text{cont}}$, there may be a region where sufficiently dense baryonic matter has the same symmetries as quark matter, and there need not be any phase transition between them.

Color-flavor locking will always occur for sufficiently large chemical potential, for any nonzero, finite m_s . This follows from Son’s model-independent analysis valid at very high densities.(9) As a consequence of color-flavor locking, chiral

symmetry is spontaneously broken even at asymptotically high densities, in sharp contrast to the well established restoration of chiral symmetry at high temperature.

Finally, it is interesting to ask what we expect at non-zero temperature. There has been no comprehensive NJL study of this, but one can make the reasonable guess that quark pairing with a gap Δ at $T = 0$ will disappear in a phase transition at $T_c \approx 0.6\Delta$. This is the BCS result, which is also found to hold for quark pairing (13, 12).

Assuming the zero-temperature phase structure given in Figure 4, we can guess that the non-zero temperature μ - T phase diagram for strange quark masses varying from infinity to zero will be as shown in the diagrams of Figure 5. These are assembled into a single three-dimensional diagram in Figure 6, where for clarity only the chiral phase transition surface is shown: the thick red line is tricritical, and the red shaded region that it bounds is second-order.

The main features of the phase diagram are as follows.

- The second-order chiral phase transition (dashed line) that is present at low density and high temperature shrinks as the strange quark becomes lighter, until at $m_s = m_s^*$ the tricritical point arrives at $T = 0$. At lower masses, there is no second-order line.
- The strangeness-breaking line (green) and the high-density chiral symmetry breaking line (red) do not exactly coincide because at low enough temperature there is a window of densities where strange quarks are present, but their Fermi momentum is too low to allow them to pair with the light quarks. This is the 2SC+s phase, where the strange quarks pair with themselves, breaking strangeness/baryon number, in a color-spin locked phase whose gap and critical temperature are very small (43).
- At arbitrarily high densities, where the QCD gauge coupling is small, quark matter is always in the CFL phase with broken chiral symmetry. This is true independent of whether the “transition” to quark matter is continuous, or whether, as for larger m_s , there are two first order transitions, from nuclear matter to the 2SC phase, and then to the CFL phase.
- Color-flavor locking survives for $M_s^2 \lesssim 2\sqrt{2}\mu\Delta$ (see below). Since the CFL state is \tilde{Q} -neutral, there are no electrons present in this phase (47), so introducing electromagnetism makes no difference to it.

Additional features, beyond those required by symmetry considerations alone, have been suggested by Pisarski (48), by analogy with scalar-gauge field theories.

4.2 Quark-hadron continuity

The pink region in Figure 4 is characterized by a definite global symmetry, $SU(2) \times [U(1)]$, but this can either be a hadronic (hyperonic) phase with unbroken isospin and electromagnetism, or a color-flavor locked quark matter phase with an isospin+color symmetry and a rotated electromagnetism that allows a linear combination of the photon and a gluon to remain massless. In other words, in this regime there is no symmetry difference between hyperonic matter and quark

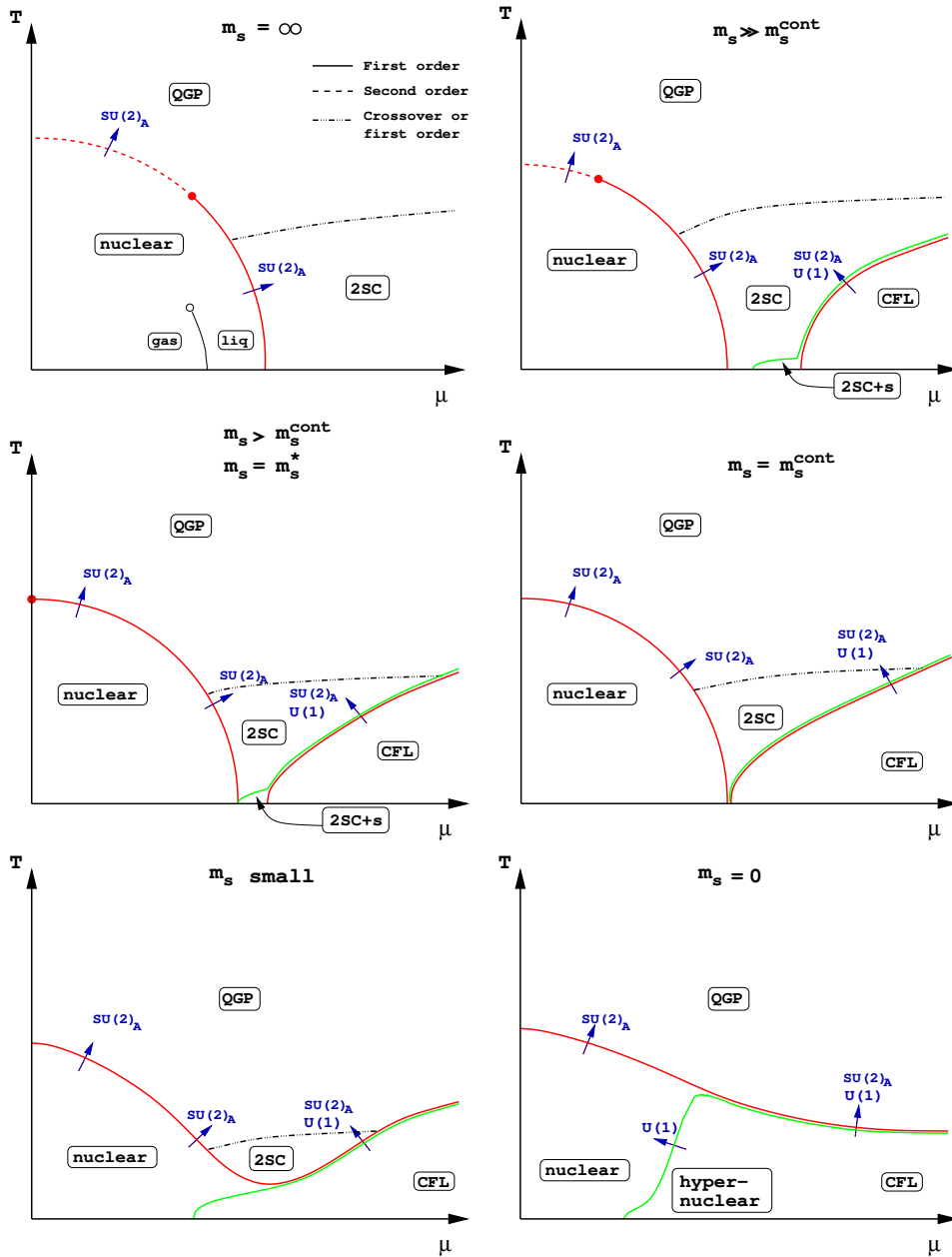


Figure 5: The phases of QCD in the chemical potential and temperature plane, for various strange quark masses, interpolating from the two flavor to the three flavor theory. The up and down quark masses and electromagnetism are neglected. Lines of breaking of $SU(2)$ chiral symmetry and $U(1)$ strangeness are shown. The QGP and 2SC phases have the same global symmetries, so the dot-dash line separating them represents the possibility of first order transitions that become crossovers at critical points.

matter. This raises the exciting possibility (35) that properties of sufficiently dense hadronic matter could be found by extrapolation from the quark matter regime where weak-coupling methods can be used.

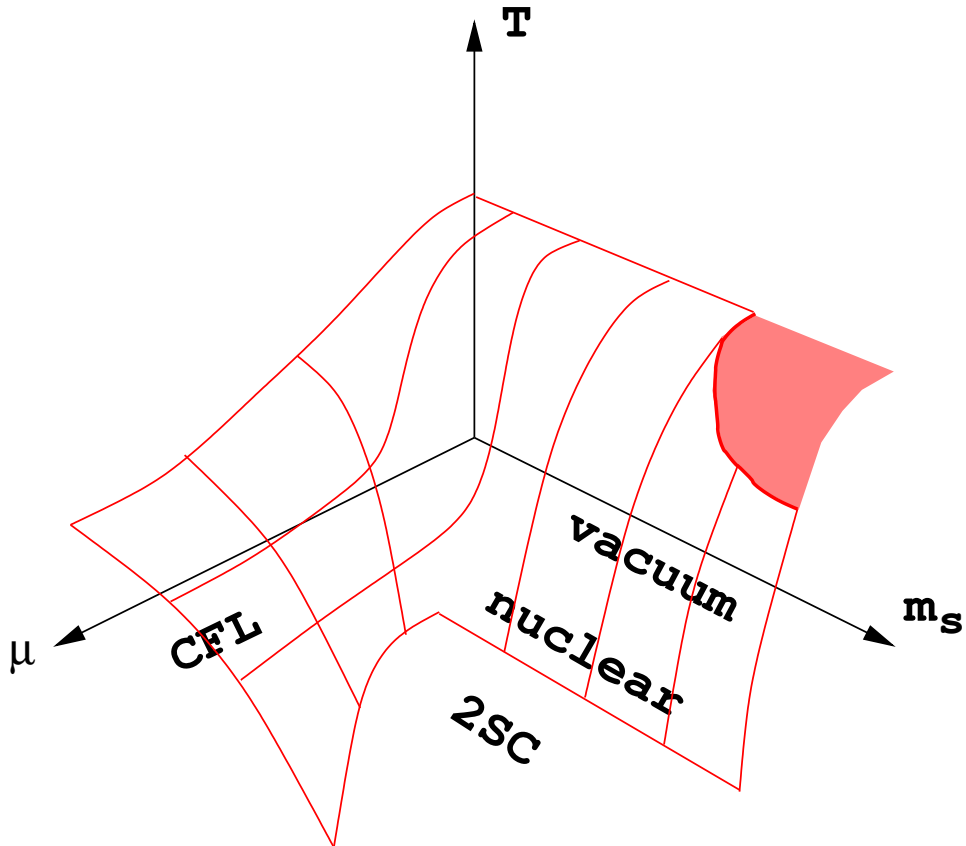


Figure 6: The chiral phase transition surface as a function of chemical potential μ , strange quark mass m_s , and temperature T . The diagrams of Figure 5 are a sequence of μ - T sections through this space. The shaded region at high m_s and T is the second-order part of the critical surface, which is bounded by a tricritical line. Everywhere else the phase transition is conjectured to be first-order.

Table 2: Quark hadron continuity: mapping between states in high density hadronic and quark matter.

Particle type	Hyperonic matter	\Leftrightarrow	CFL quark matter
Fermions:	8 Baryons	\Leftrightarrow	9 Quarks
Chiral (pseudo)Goldstone:	8 pion/kaons	\Leftrightarrow	8 pseudoscalars
Baryon number (pseudo)Goldstone:	1	\Leftrightarrow	1
Vector Mesons:	9	\Leftrightarrow	8 massive gluons

The most straightforward application of this idea is to relate the quark/gluon description of the spectrum to the hadron description of the spectrum in the CFL phase.(35) The conjectured mapping is given in Table 2. Gluons in the CFL phase map to the octet of vector bosons; the Goldstone bosons associated with chiral symmetry breaking in the CFL phase map to the pions; and the quarks map onto baryons. Pairing occurs at the Fermi surfaces, and we therefore expect the gap parameters in the various quark channels to map to the gap parameters

due to baryon pairing.

Table 3: Mapping of fermionic states between high density quark and hadronic matter.

Quark	$SU(2)_{\text{color}+V}$	\tilde{Q}	Hadron	$SU(2)_V$	Q
$\begin{pmatrix} bu \\ bd \end{pmatrix}$	2	+1 0	$\begin{pmatrix} p \\ n \end{pmatrix}$	2	+1 0
$\begin{pmatrix} gs \\ rs \end{pmatrix}$	2	0 -1	$\begin{pmatrix} \Xi^0 \\ \Xi^- \end{pmatrix}$	2	0 -1
$\begin{pmatrix} ru - gd \\ gu \\ rd \end{pmatrix}$	3	0 +1 -1	$\begin{pmatrix} \Sigma^0 \\ \Sigma^+ \\ \Sigma^- \end{pmatrix}$	3	0 +1 -1
$ru + gd + \xi_- bs$	1	0	Λ	1	0
$ru + gd - \xi_+ bs$	1	0	—		

In Table 3 we show how this works for the fermionic states in 2+1 flavor QCD. There are nine states in the quark matter phase. We show how they transform under the unbroken “isospin” of $SU(2)_{\text{color}+V}$ and their charges under the unbroken “rotated electromagnetism” generated by \tilde{Q} , as described in Section 4. Table 3 also shows the baryon octet, and their transformation properties under the symmetries of isospin and electromagnetism that are unbroken in sufficiently dense hadronic matter. Clearly there is a correspondence between the two sets of particles.¹ As μ increases, the spectrum described in Table 2 may evolve continuously even as the language used to describe it changes from baryons, $SU(2)_V$ and Q to quarks, $SU(2)_{\text{color}+V}$ and \tilde{Q} .

If the spectrum changes continuously, then in particular so must the gaps. As discussed above, the quarks pair into rotationally invariant, \tilde{Q} -neutral, $SU(2)_{\text{color}+V}$ singlets. The two doublets of Table 3 pair with each other, the triplet pairs with itself. Finally, the two singlets pair with themselves.

5 COLOR-FLAVOR UNLOCKING AND THE CRYSTALLINE COLOR SUPERCONDUCTING PHASE

A prominent feature of the zero temperature phase diagram Figure 4 is the “unlocking” phase transition between two-flavor pairing (2SC) and three-flavor pairing (CFL). At this phase transition, the Fermi momentum of free strange quarks is sufficiently different from that of the light quarks to disrupt pairing between them.

Such transitions are expected to be a generic feature of quark matter in nature. In the absence of interactions, the requirements of weak equilibrium and charge neutrality cause all three flavors of quark to have different Fermi momenta. In the

¹The one exception is the final isosinglet. In the $\mu \rightarrow \infty$ limit, where the full 3-flavor symmetry is restored, it becomes an $SU(3)$ singlet, so it is not expected to map to any member of the baryon octet. The gap Δ_+ in this channel is twice as large as the others.

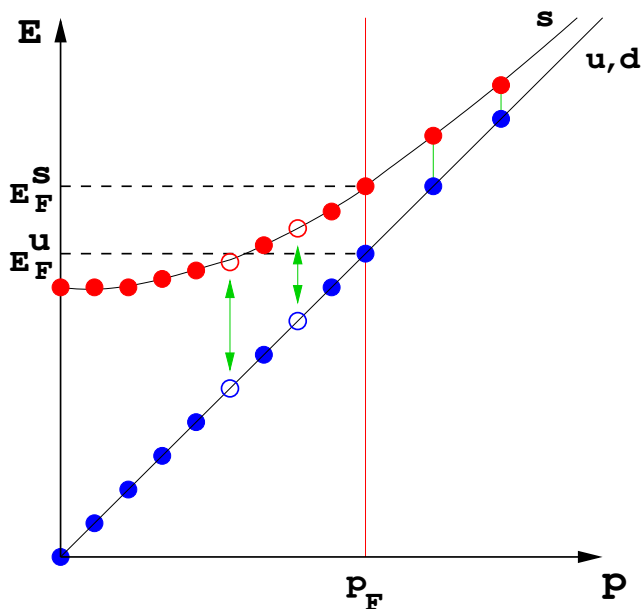


Figure 7: How the strange quark mass interferes with a u - s condensate. The strange quark (upper curve) and light quark (straight line) dispersion relations are shown, with their Fermi seas filled up to a common Fermi momentum p_F . The horizontal axis is the magnitude of the spatial momentum; s -wave pairing occurs between particles (or holes) with the same p and opposite \vec{p} . The energy gained by pairing stops the s quarks from decaying to u quarks (see text).

extreme case where all three flavors had very different chemical potentials, each flavor would have to self-pair (49, 43), but in the phenomenologically interesting density range we expect a rich and complex phase structure for cold dense matter as a function of quark masses and density. The CFL \leftrightarrow 2SC transition of Figure 4 is one example. Assuming that no other intermediate phases are involved, we now give a model independent argument that the unlocking phase transition between the CFL and 2SC phases in Figure 4 must be first order. However, there is good reason to expect an intermediate state—the crystalline color superconducting state, and we go on to discuss it in some detail. Note that another crystalline phase, the “chiral crystal” has also been proposed (50), although it is not yet clear whether there is any window of density where it is favored.

5.1 The (un)locking transition

Figure 7 shows part of the CFL pairing pattern: the quark states of the different flavors are filled up to a common Fermi momentum $p_F \approx \mu$, intermediate between the free light quark and free strange quark Fermi momenta. In the absence of interactions, this state would be unstable: weak interactions would turn strange quarks into light quarks, and there would be separate strange and light Fermi momenta, each filled up to the Fermi energy μ . However, pairing stabilizes it.

For the paired state to be stable, it must be that the free energy gained from turning a strange quark into a light quark is less than the energy lost by breaking the Cooper pairs for the modes involved (47).

$$\sqrt{\mu^2 + M_s(\mu)^2} - \sqrt{\mu^2 + M_u(\mu)^2} \approx \frac{M_s(\mu)^2 - M_u(\mu)^2}{2\mu} \lesssim 2\Delta_{us} , \quad (11)$$

i.e., $\frac{M_s(\mu)^2}{4\mu} \lesssim \Delta_{us}$

Here $M_s(\mu)$ and $M_u(\mu)$ are the constituent quark masses in the CFL phase, and $M_u(\mu) \ll M_s(\mu)$. An additional factor of $1/\sqrt{2}$ on the RHS of (11) can be obtained requiring the paired state to have lower free energy (51,52,47). Equation (11) implies that arbitrarily small values of Δ_{us} are impossible, which means that the phase transition must be first-order: the gap cannot go continuously to zero. Such behavior has been found in calculations for unlocking phase transitions of this kind in electron superconductors (51) and nuclear superfluids (53) as well as QCD superconductors (38, 54, 55).

5.2 The crystalline color superconducting phase

There is good reason to think that, in the region where the strange quark is just on the edge of decoupling from the light quarks, another form of pairing can occur. This is the ‘‘LOFF’’ state, first explored by Larkin and Ovchinnikov (56) and Fulde and Ferrell (57) in the context of electron superconductivity in the presence of magnetic impurities. They found that near the unpairing transition, it is favorable to form a state in which the Cooper pairs have nonzero momentum. This is favored because it gives rise to a region of phase space where each of the two quarks in a pair can be close to its Fermi surface, and such pairs can be created at low cost in free energy. Condensates of this sort spontaneously break translational and rotational invariance, leading to gaps which vary periodically in a crystalline pattern. The possible consequences for compact stars will be discussed in section 6.

In Ref. (52), the LOFF phase in QCD has been studied using a toy model in which the quarks interact via a four-fermion interaction with the quantum numbers of single gluon exchange. The model only considers pairing between u and d quarks, with $\mu_d = \bar{\mu} + \delta\mu$ and $\mu_u = \bar{\mu} - \delta\mu$. For the rest of this section we will discuss properties of the model, but it is important to remember that in reality we expect a LOFF state wherever the difference between the Fermi momenta of any two quark flavors is near an unpairing transition, for example the unlocking phase transition between the 2SC and CFL phases.

5.2.1 The nature of LOFF pairing

Whereas the BCS state requires pairing between fermions with equal and opposite momenta, for some values of $\delta\mu$ it may be more favorable to form a condensate of Cooper pairs with *nonzero* total momentum. By pairing quarks with momenta which are not equal and opposite, some Cooper pairs are allowed to have both the up and down quarks on their respective Fermi surfaces even when $\delta\mu \neq 0$.

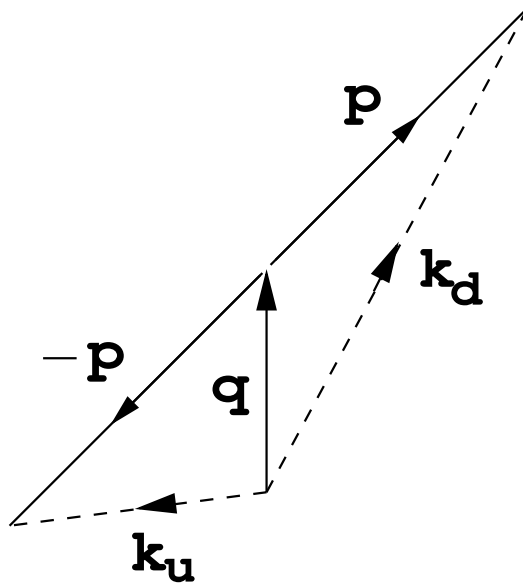


Figure 8: The momenta \mathbf{k}_u and \mathbf{k}_d of the two members of a LOFF-state Cooper pair. We choose the vector \mathbf{q} , common to all Cooper pairs, to coincide with the z -axis.

LOFF found that within a range of $\delta\mu$ a condensate of Cooper pairs with momenta $\mathbf{k}_u = \mathbf{q} + \mathbf{p}$ and $\mathbf{k}_d = \mathbf{q} - \mathbf{p}$ (see Figure 8) is favored over either the BCS condensate or the normal state. Here, our notation is such that \mathbf{p} specifies a particular Cooper pair, while \mathbf{q} is a fixed vector, the same for all pairs, which characterizes a given LOFF state. The magnitude $|\mathbf{q}|$ is determined by minimizing the free energy; the direction of \mathbf{q} is chosen spontaneously. The resulting LOFF state breaks translational and rotational invariance. In position space, it describes a condensate which varies as a plane wave with wave vector $2\mathbf{q}$.

5.2.2 Results from a simplified model

In the LOFF state, each Cooper pair carries momentum $2\mathbf{q}$, so the condensate and gap parameter vary in space with wavelength $\pi/|\mathbf{q}|$. In the range of $\delta\mu$ where the LOFF state is favored, $|\mathbf{q}| \approx 1.2\delta\mu$. In Ref. (52), we simplify the calculation of the gap parameter by assuming that the condensate varies in space like a plane wave, leaving the determination of the crystal structure of the QCD LOFF phase to future work. We make an ansatz for the LOFF wave function, and by variation obtain a gap equation which allows us to solve for the gap parameter Δ_A , the free energy and the values of the diquark condensates which characterize the LOFF state at a given $\delta\mu$ and $|\mathbf{q}|$. We then vary the momentum $|\mathbf{q}|$ of the ansatz, to find the preferred (lowest free energy) LOFF state at a given $\delta\mu$, and compare the free energy of the LOFF state to that of the BCS state with which it competes. We show results for one choice of parameters in Figure 9(a).

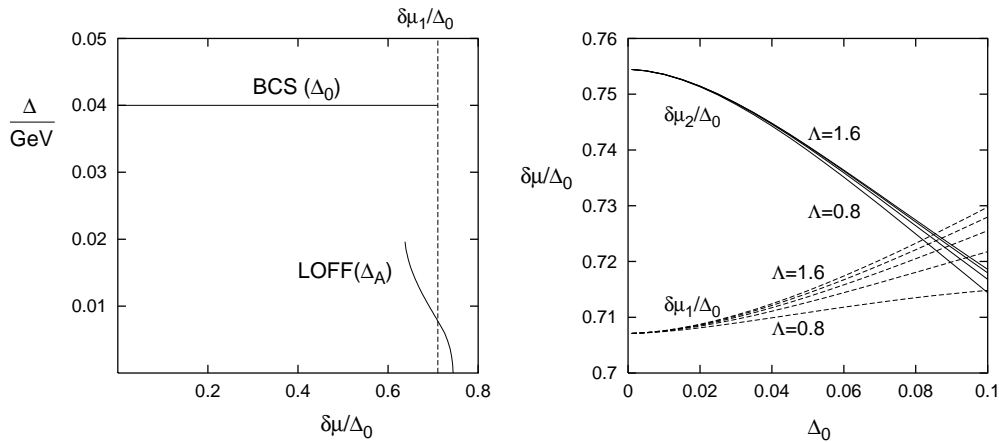


Figure 9: (a) LOFF and BCS gap parameters as a function of $\delta\mu$, with coupling chosen so that $\Delta_0 = 40$ MeV, and $\Lambda = 1$ GeV. The vertical dashed line marks $\delta\mu = \delta\mu_1$, above which the LOFF state has lower free energy than BCS. (b) The interval of $\delta\mu$ within which the LOFF state occurs as a function of the coupling, parametrized by the BCS gap Δ_0 in GeV. Below the solid line, there is a LOFF state. Below the dashed line, the BCS state is favored. The different lines of each type correspond to different cutoffs on the four-fermion interaction: $\Lambda = 0.8$ GeV to 1.6 GeV. $\delta\mu_1/\Delta_0$ and $\delta\mu_2/\Delta_0$ show little cutoff-dependence, and the cutoff dependence disappears completely as $\Delta_0, \delta\mu \rightarrow 0$.

In Figure 9 the average quark chemical potential $\bar{\mu}$ has been set to 0.4 GeV, corresponding to a baryon density of about 4 to 5 times that in nuclear matter. A crude estimate (52) suggests that in quark matter at this density, $\delta\mu \sim 15 - 30$ MeV depending on the value of the density-dependent effective strange quark mass.

We find that the LOFF state is favored for values of $\delta\mu$ which satisfy $\delta\mu_1 < \delta\mu < \delta\mu_2$ as shown in Figure 9(b), with $\delta\mu_1/\Delta_0 = 0.707$ and $\delta\mu_2/\Delta_0 = 0.754$ in the weak coupling limit $\Delta_0 \ll \mu$. (Δ_0 is the 2SC gap for $\delta\mu < \delta\mu_1$, and one can use it to parametrize the strength of the four fermion interaction G : small Δ_0 corresponds to a small G .) At weak coupling, the LOFF gap parameter decreases from $0.23\Delta_0$ at $\delta\mu = \delta\mu_1$ (where there is a first order BCS-LOFF phase transition) to zero at $\delta\mu = \delta\mu_2$ (where there is a second order LOFF-normal transition). Except for very close to $\delta\mu_2$, the critical temperature above which the LOFF state melts will be much higher than typical neutron star temperatures. At stronger coupling the LOFF gap parameter decreases relative to Δ_0 and the window of $\delta\mu/\Delta_0$ within which the LOFF state is favored shrinks, as seen in Figure 9(b).

5.2.3 General properties of the LOFF phase

The LOFF state is characterized by a gap parameter Δ_A and a diquark condensate, but not by an energy gap in the dispersion relation. Because the condensate breaks rotational invariance, the quasiparticle dispersion relations vary with the direction of the momentum, yielding gaps that vary from zero up to a maximum of Δ_A .

Near the second-order critical point $\delta\mu_2$, we can describe the phase transition with a Ginzburg-Landau effective potential. The order parameter for the LOFF-to-normal phase transition is

$$\Phi(\mathbf{r}) = -\frac{1}{2}\langle\epsilon_{ab}\epsilon_{\alpha\beta\gamma}\psi^{a\alpha}(\mathbf{r})C_{\gamma 5}\psi^{b\beta}(\mathbf{r})\rangle \quad (12)$$

so that in the normal phase $\Phi(\mathbf{r}) = 0$, while in the LOFF phase $\Phi(\mathbf{r}) = \Gamma_A e^{i2\mathbf{q}\cdot\mathbf{r}}$. (The gap parameter is related to the order parameter by $\Delta_A = G\Gamma_A$.) Expressing the order parameter in terms of its Fourier modes $\tilde{\Phi}(\mathbf{k})$, we write the LOFF free energy (relative to the normal state) as

$$F(\{\tilde{\Phi}(\mathbf{k})\}) = \sum_{\mathbf{k}} \left(C_2(k^2)|\tilde{\Phi}(\mathbf{k})|^2 + C_4(k^2)|\tilde{\Phi}(\mathbf{k})|^4 + \mathcal{O}(|\tilde{\Phi}|^6) \right). \quad (13)$$

For $\delta\mu > \delta\mu_2$, all of the $C_2(k^2)$ are positive and the normal state is stable. Just below the critical point, all of the modes $\tilde{\Phi}(\mathbf{k})$ are stable except those on the sphere $|\mathbf{k}| = 2q_2$, where q_2 is the value of $|\mathbf{q}|$ at $\delta\mu_2$ (so that $q_2 \simeq 1.2\delta\mu_2 \simeq 0.9\Delta_0$ at weak coupling). In general, many modes on this sphere can become nonzero, giving a condensate with a complex crystal structure. We consider the simplest case of a plane wave condensate where only the one mode $\tilde{\Phi}(\mathbf{k} = 2\mathbf{q}_2) = \Gamma_A$ is nonvanishing. Dropping all other modes, we have

$$F(\Gamma_A) = a(\delta\mu - \delta\mu_2)(\Gamma_A)^2 + b(\Gamma_A)^4 \quad (14)$$

where a and b are positive constants. Finding the minimum-energy solution for $\delta\mu < \delta\mu_2$, we obtain simple power-law relations for the condensate and the free energy:

$$\Gamma_A(\delta\mu) = K_\Gamma(\delta\mu_2 - \delta\mu)^{1/2}, \quad F(\delta\mu) = -K_F(\delta\mu_2 - \delta\mu)^2. \quad (15)$$

These expressions agree well with the numerical results obtained by solving the gap equation (52). The Ginzburg-Landau method does not specify the proportionality factors K_Γ and K_F , but analytical expressions for these coefficients can be obtained in the weak coupling limit by explicitly solving the gap equation (58, 52).

Notice that because $(\delta\mu_2 - \delta\mu_1)/\delta\mu_2$ is small, the power-law relations (15) are a good model of the system throughout the entire LOFF interval $\delta\mu_1 < \delta\mu < \delta\mu_2$ where the LOFF phase is favored over the BCS phase. The Ginzburg-Landau expression (14) gives the free energy of the LOFF phase near $\delta\mu_2$, but it cannot be used to determine the location $\delta\mu_1$ of the first-order phase transition where the LOFF window terminates, which requires a comparison of LOFF and BCS free energies.

6 COMPACT STAR PHENOMENOLOGY

Having described the interesting phenomena that we believe occur in cold quark matter, we now ask ourselves where in nature such phenomena might occur, and how we might see evidence of them.

The only place in the universe where we expect sufficiently high densities and low temperatures is compact stars, also known as “neutron stars”, since it is often assumed that they are made primarily of neutrons (for a recent review, see (59)). A compact star is produced in a supernova. As the outer layers of the star are blown off into space, the core collapses into a very dense object. Typical compact stars have masses close to $1.4M_{\odot}$, and are believed to have radii of order 10 km. The density ranges from around nuclear density near the surface to higher values further in, although uncertainty about the equation of state leaves us unsure of the value in the core.

During the supernova, the core collapses, and its gravitational energy heats it to temperatures of order 10^{11} K (tens of MeV), but it cools rapidly by neutrino emission. Within a few minutes its internal temperature T drops to 10^9 K (100 keV), and reaches 10^7 K (1 keV) after a century. Neutrino cooling continues to dominate for the first million years of the life of the star. The effective temperature T_e of the X-ray emissions is lower than the internal temperature: $T_e/10^6 \text{ K} \approx \sqrt{T/10^8 \text{ K}}$ (60).

Color superconductivity gives mass to excitations around the ground state: it opens up a gap at the quark Fermi surface, and makes the gluons massive. One would therefore expect its main consequences to relate to transport properties, such as mean free paths, conductivities and viscosities. The influence of color superconductivity on the equation of state is an $\mathcal{O}((\Delta/\mu)^2)$ (few percent) effect, which is not phenomenologically interesting given the existing uncertainty in the equation of state at the relevant densities.

6.1 Cooling by neutrino emission

As mentioned above, for its first million or so years, a neutron star cools by neutrino emission. The temperature is obtained from X-ray spectra of isolated compact stars, and is subject to many uncertainties, including emissions from plasma around the star, and distortion of the spectrum by a possible hydrogen atmosphere. The age, inferred from the spindown rate by assuming magnetic dipole radiation from a constant dipole moment, may also have large systematic errors. Even so, a consistent picture emerges (61, 60) in which the youngest compact stars, about a thousand years old, have surface temperatures around 2×10^6 K (200 eV), falling to about 3×10^5 K (30 eV) after a million years.

The cooling rate is determined by the heat capacity and emissivity, both of which are dominated by quark modes whose energy is within T of the Fermi surface, and are therefore sensitive to the kind of gaps generated by color superconductivity (61, 62, 60).

In the CFL phase, all quarks and gluons have gaps $\Delta \gg T$, electrons are absent (47), and the transport properties are dominated by the only true Goldstone excitation, the superfluid mode arising from the breaking of the exact baryon number symmetry. The next lightest modes are the pseudo-Goldstone bosons associated with chiral symmetry breaking, which will only participate when the temperature is above their mass, which is of order tens of MeV (63). This means that CFL quark matter has a much smaller neutrino emissivity and heat capacity than nuclear matter, and hence the cooling of a neutron star is likely to be

dominated by the nuclear mantle rather than the CFL core (60). A CFL core is therefore not detectable by cooling measurements.

We turn now to the 2SC quark matter phase, which occurs if the strange quarks are too heavy to pair with the light flavors. Up and down quarks of two of the colors (red and green, say) pair strongly with a gap much bigger than the temperature. This leaves the blue up and down, and the strange quarks (if present) with much more weakly attractive channels in which to pair. The strange quarks are believed to pair with each other in a “color-spin locked” condensate, with a gap of order hundreds of keV (43) or less (52). The blue up and down quarks form $J = 1$ pairs, breaking rotational invariance (7), with a gap that was originally estimated to be in the keV range, but this estimate is not robust, and depends on details of the NJL model used (7).

This leads to potentially interesting phenomenology, since the blue and/or strange quarks have small gaps, so during the early life of the compact star they may participate in the cooling dynamics as long as the temperature is greater than their gap. Their effects would be dramatic, allowing high rates of neutrino emission via direct URCA processes such as $d \rightarrow u + e + \bar{\nu}$ and $u \rightarrow d + e^+ + \nu$, and leading to rapid cooling of the core (61, 60). The cooling would slow down suddenly when the temperature fell below the gap. Such a behavior would be observable, and if no sign of it is seen as our observations of neutron star temperatures improve then we will have to conclude that either 2SC matter does not occur, or the smallest gaps are larger than the observed temperatures.

6.2 *The neutrino pulse at birth*

We have seen above that in the first seconds of a supernova, the inner regions (“protonneutron star”) are heated to tens of MeV by the gain a vast amount of energy from the gravitational collapse, and are consequently hot (tens of MeV). Over the next half-minute or so much of the energy is radiated off as neutrinos, whose detailed spectrum as a function of time is determined by the neutrino diffusion properties of the protonneutron star. Neutrinos from supernova 1987A were detected in terrestrial experiments, and the duration and mean energy of the pulse was measured. We can hope that neutrinos from future supernovae in our galaxy will be measured more precisely. It is therefore useful to study the effects of color superconductivity on neutrino diffusion, in order to see if it leads to any signature in the neutrino pulse.

Carter and Reddy (64) have performed a preliminary investigation of this question. They restricted themselves to two flavors, and studied the case where the core starts off as a hot quark-gluon plasma. Within seconds, thanks to neutrino emission, it cools into a superconducting phase, and they assumed that this occurred via a second-order phase transition. This leads to a striking two-stage signature: (1) near the critical temperature T_c the heat capacity rises, and the cooling of the star consequently slows; (2) below the critical temperature, the quark modes are gapped, and the neutrino mean free path is enhanced by $\exp(\Delta/T)$, reflecting Boltzmann suppression of the population of quark quasi-particles. As a result, the core may suddenly empty itself of neutrinos, creating a final neutrino burst. There may be further processing of this burst on its way out

of the supernova, but the suggestion is that it may survive to yield a noticeable signal in neutrino detectors on earth. The suggestion, then, is that the flux of supernova neutrinos detected on earth will not taper off, but show a final burst followed by no flux. Before that, there may be a plateau in the energy or flux of the neutrinos, as the cooling slows near the critical temperature.

There are many issues that require further investigation. It is not clear whether a second-order phase transition is to be expected, since the up and down quark Fermi surfaces will differ, and there may be a first-order unlocking transition (55). Also, it is necessary to take into account the strange quark, and the processing of emitted neutrinos by the layers of neutrino-opaque hadronic matter that surround the core during the supernova explosion.

6.3 r -mode instability

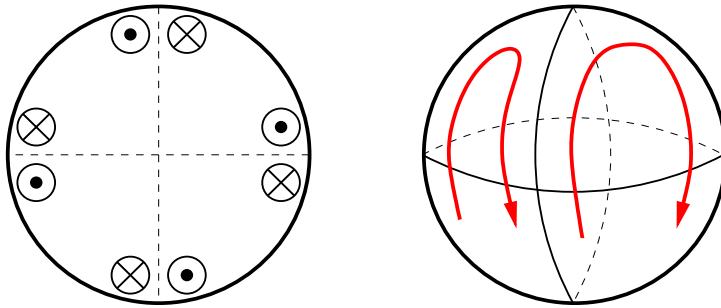


Figure 10: The quadrupole pattern of r -mode bulk flows

The term “ r -mode” (short for “rotational mode”) refers to a bulk flow in a rotating star that radiates away energy and angular momentum in the form of gravitational waves (Figure 10). If the rotation frequency f of the star is above a critical value f_* , the system becomes unstable to r -modes and will quickly spin down until its frequency drops to f_* , at which point the r -modes are damped out. The critical frequency depends on the sources of damping that could suppress the flows. These include shear and bulk viscosities, and also “surface rubbing”—the friction at the interface between the r -mode region and any rigid crust that cannot flow. Since the viscosities are sensitive functions of temperature, one calculates $f_*(T)$ as an upper limit on rotation frequencies, and thereby maps out an excluded high- f region in the T - f plane. Differently constituted compact stars (neutrons, quarks with various gaps due to pairing) have different excluded regions, and one can see whether any of them are ruled out by the observation of pulsars in nature with rotation rates and temperatures in their excluded region.

Madsen (65) has shown that gapless quark matter and neutron stars are not ruled out. However, color superconductivity creates gaps in the quark excitation spectrum, suppressing the viscosities by factors of order $\exp(-\Delta/T)$, and encouraging r -mode spindown. He found that for a compact star made *entirely* of quark matter in the CFL phase, even a quark gap as small as $\Delta = 1$ MeV reduces $f_*(T)$ dramatically to $\mathcal{O}(100$ Hz) for temperatures below 10^9 K (100 keV). This

means that millisecond pulsars, with frequencies up to 640 Hz, cannot be CFL quark matter stars, making it questionable whether any compact stars are made entirely of CFL quark matter. Madsen found that 2SC quark matter stars were on the edge of being ruled out, so he was not able to say anything about them, either positive or negative.

Madsen included the additional damping from surface rubbing between the quark matter and a normal matter crust. Using the conventional picture, this is a very small effect, since the crust is separated from the quark matter by an electrostatic cushion of electrons, and so surface rubbing made no difference to the result for pure CFL stars. Actually, since CFL matter is neutral (47), it contains no electrons, so the cushioning mechanism may not be operative, and it is not clear that there is any such crust.

There are caveats to Madsen's conclusions. Firstly, the results are sensitive to the temperature of the inner regions of the star, which has to be inferred from the measured effective surface temperature using models of the heat flow, and is therefore not accurately known. However, this uncertainty is only important for unpaired or 2SC paired quark matter; pure CFL stars are ruled out for $T_e < 10^9$ K (100 keV), which is already at the upper end of conceivable temperatures. Secondly, as he points out, his calculations do not rule out the generic picture of how quark matter occurs in compact stars, namely as a quark matter core surrounded by a nuclear mantle. In this case substantial friction is expected at the core-mantle interface, and this may be enough (66,65) to stabilize the star irrespective of the viscosities of the quark matter. Furthermore, quark matter may contain a shell of LOFF crystal (see below), and the r -modes could be damped at the edges of that region rather than at the crust. We can hope that future work on hybrid stars will clarify the situation.

6.4 *Magnetic field decay*

The behavior of magnetic fields in quark matter is quite different from that in nuclear matter (67,68). Nuclear matter is an electromagnetic superconductor (because of proton-proton pairing which breaks the $U(1)_Q$ gauge symmetry) and also a superfluid (because of neutron-neutron pairing). Magnetic fields are therefore restricted to Abrikosov flux tubes, and angular momentum is carried by rotational vortices. The magnetic flux tubes can be dragged about by the outward motion of the rotational vortices as the neutron star spins down (69,70,71,72,73), and can also be pushed outward if the gap at the proton fermi surface increases with depth within the neutron star (74). One therefore expects the magnetic field of an isolated pulsar to decay over billions of years as it spins down (70,71,72,73) or perhaps more quickly (74). However, there is no observational evidence for the decay of the magnetic field of an isolated pulsar over periods of billions of years (71,75).

A color superconductor, on the other hand, leaves unbroken a rotated electromagnetism $U(1)_{\tilde{Q}}$, a mixture of photon and gluon, allowing long-range \tilde{Q} -magnetic fields. This is true of the CFL phase, and also of the 2SC phase as long as the temperature is high enough so that the blue quarks do not pair.

The new unbroken rotated electromagnetic field $A_{\tilde{Q}}$ is just a linear combination

of the photon A_μ and one of the gluons G_μ^8 ,

$$A_\mu^{\tilde{Q}} = \cos \alpha_0 A_\mu + \sin \alpha_0 G_\mu^8 \quad (16)$$

the orthogonal combination A_μ^X is massive. The mixing angle α_0 is the analogue of the Weinberg angle in electroweak theory, in which the presence of the Higgs condensate causes the hypercharge and W_3 gauge bosons to mix to form the photon, A_μ , and the massive Z boson. $\sin(\alpha_0)$ is proportional to e/g and turns out to be about $1/20$ in the 2SC phase and $1/40$ in the CFL phase (68). This means that the \tilde{Q} -photon which propagates in color superconducting quark matter is mostly photon with only a small gluon admixture. If a color superconducting neutron star core is subjected to an ordinary magnetic field, it will either expel the X component of the flux or restrict it to flux tubes, but it admits the great majority of the flux in the form of a $B_{\tilde{Q}}$ magnetic field satisfying Maxwell's equations. The decay in time of this "free field" (i.e. not in flux tubes) is limited by the \tilde{Q} -conductivity of the quark matter.

The CFL phase contains no electrons, and all its charged modes are gapped, making it an electromagnetic insulator. The 2SC phase has electrons as well as blue quasi-quarks, and turns out to be a very good conductor. Thus the 2SC and CFL phases, while both allowing long-range \tilde{Q} -flux fields, react very differently to attempts to *change* the magnetic field. The CFL phase allows such changes, but the 2SC, as a near-perfect conductor, generates eddy currents that oppose the change, locking the magnetic field into the core with a decay time of order 10^{13} years (68)

This means that a 2SC quark matter core within a neutron star can act as an "anchor" for the magnetic field, preventing the flux-tube-dragging mechanism that can operate in ordinary nuclear matter. Even though this distinction is a qualitative one, it will be difficult to confront it with data since what is observed is the total dipole moment of the neutron star. A color superconducting core can only anchor those magnetic flux lines which pass through the core, while in a neutron star with no quark matter core the entire internal magnetic field can decay over time. In both cases, however, the total dipole moment can change since the magnetic flux lines which do not pass through the core can move.

6.5 Glitches and the crystalline color superconductor

The crystalline LOFF phase has been discussed above. It occurs when two different types of quark have different Fermi momenta (because their masses or chemical potentials are different) and are just barely able to pair.

Such situations are likely to be generic in nature, where, because of the strange quark mass, combined with requirements of weak equilibrium and charge neutrality, all three flavors of quark in general have different chemical potentials. To date the LOFF condensate has only been studied in simplified two-flavor models, so it is not clear whether it can be expected to occur in compact stars. However, in the model a LOFF phase occurred if the gap Δ_0 which characterizes the uniform color superconductor present at smaller values of $\delta\mu$ was about 40 MeV (52). This is in the middle of the range of present estimates of superconducting gaps. It is therefore worthwhile to consider the consequences.

6.5.1 Glitches and vortex pinning

Glitches are sudden jumps in rotation frequency Ω of a pulsar, which may be as large as $\Delta\Omega/\Omega \sim 10^{-6}$, but may also be several orders of magnitude smaller. The frequency of observed glitches is statistically consistent with the hypothesis that all radio pulsars experience glitches (76). Glitches are thought to originate in the rigid neutron star crust, typically somewhat more than a kilometer thick, where rotational vortices in a neutron superfluid are pinned to the crystal structure of the crust. As the pulsar's spin gradually slows, the vortices must gradually move outwards since the rotation frequency of a superfluid is proportional to the density of vortices. Models (77) differ in important respects as to how the stress associated with pinned vortices is released in a glitch: for example, the vortices may break and rearrange the crust, or a cluster of vortices may suddenly overcome the pinning force and move macroscopically outward, with the sudden decrease in the angular momentum of the superfluid within the crust resulting in a sudden increase in angular momentum of the rigid crust itself and hence a glitch. All the models agree that the fundamental requirements are the presence of rotational vortices in a superfluid and the presence of a rigid structure which impedes the motion of vortices and which encompasses enough of the volume of the pulsar to contribute significantly to the total moment of inertia.

Henceforth, we suppose that the LOFF phase is a superfluid, which means that if it occurs within a pulsar it will be threaded by an array of rotational vortices. It is reasonable to expect that these vortices will be pinned in a LOFF crystal, in which the diquark condensate varies periodically in space. Indeed, one of the suggestions for how to look for a LOFF phase in terrestrial electron superconductors relies on the fact that the pinning of magnetic flux tubes (which, like the rotational vortices of interest to us, have normal cores) is expected to be much stronger in a LOFF phase than in a uniform BCS superconductor (78). Note that the chiral crystal phase (50) is not a superfluid, so it will not contain rotational vortices.

6.5.2 Vortex pinning in the LOFF phase

A real calculation of the pinning force experienced by a vortex in a crystalline color superconductor must await the determination of the crystal structure of the LOFF phase. We can, however, attempt an order of magnitude estimate along the same lines as that done by Anderson and Itoh (79) for neutron vortices in the inner crust of a neutron star. In that context, this estimate has since been made quantitative (80, 81, 77). For one specific choice of parameters (52), the resulting pinning force per unit length of vortex was estimated essentially by dimensional analysis at

$$\text{LOFF: } f_p \sim (4 \text{ MeV})/(80 \text{ fm}^2). \quad (17)$$

It is premature to compare such a crude result to the results of serious calculations (80, 81, 77), but it is remarkable that they prove to be similar: the pinning force per unit length for neutron vortices in the inner crust is

$$\text{neutron star: } f_p \approx (1 - 3 \text{ MeV})/(200 - 400 \text{ fm}^2). \quad (18)$$

This raises the possibility that pulsars might be strange stars after all (82,83). Strange quark stars are made almost entirely of quark matter with either no hadronic matter content at all or perhaps a thin crust, of order one hundred meters thick, which contains no neutron superfluid (83,84). No successful models of glitches in the crust of a strange quark star have been proposed, indicating that pulsars are not strange stars (85,86,87). The possibility of a shell of crystalline LOFF quark matter inside a quark star revives the possibility that glitches could occur in quark stars, as a result of the pinning of quark-superfluid vortices to the LOFF crystal.

7 CONCLUSIONS

The possibility of quark pairing and color superconductivity in high-density QCD in an intriguing one. We have learnt much about the rich structure of phases that it leads to, as outlined in sections 2 to 5 above. There are many directions that remain to be explored, from new pairing structures to detailed studies of the known 2SC, 2SC+s, CFL, and LOFF phases. It has even been suggested that zero-density QCD can be understood in terms of a quark-paired condensate in combination with an adjoint chiral condensate (88).

The most pressing task, however, is to investigate the consequences of our findings for the phenomenology of neutron/quark stars, which are the only naturally occurring example of cold matter at the densities we have studied. The first steps in this directions have been described in section 6. Much theoretical work remains to be done before we can make sharp proposals for astrophysical observations that might teach us whether compact stars contain quark matter, and the nature of the quark pairing.

ACKNOWLEDGMENTS

I thank my collaborators J. Berges, J. Bowers, K. Rajagopal, F. Wilczek, and also S. Hsu, J. Madsen, S. Reddy, T. Schäfer for discussions and communications.

Literature Cited

1. Karsch F. *Nucl. Phys. (Proc. Suppl.)* 83-84:14 (2000)
2. Hong, D. hep-ph/0101025 (2001); Rajagopal K, Wilczek F. hep-ph/0011333 (2000); Schäfer T, Shuryak E. hep-ph/0010049 (2000); Rajagopal K. hep-ph/0009058 (2000); Rischke D, Pisarski R. Proceedings of the "Fifth Workshop on QCD", Villefranche, Jan. 3-7, 2000; Hsu S. hep-ph/0003140 (2000); Alford M. hep-ph/0003185 (2000);
3. Bardeen J, Cooper LN, Schrieffer JR. *Phys. Rev.* 106:162 (1957); *Phys. Rev.* 108:1175 (1957)
4. Barrois B, *Nucl. Phys.* B129:390 (1977); Frautschi S. "Proceedings of workshop on hadronic matter at extreme density", Erice 1978
5. Barrois B. "Nonperturbative effects in dense quark matter", Cal Tech PhD thesis, UMI 79-04847-mc (1979)
6. Bailin D, Love A. *Phys. Rept.* 107:325 (1984), and references therein
7. Alford M, Rajagopal K, Wilczek F. *Phys. Lett.* B422:247 (1998)
8. Rapp R, Schäfer T, Shuryak EV, Velkovsky M. *Phys. Rev. Lett.* 81:53 (1998)
9. Son DT. *Phys. Rev.* D59:094019 (1999)
10. Schäfer T, Wilczek F. *Phys. Rev.* D60:114033 (1999)
11. Pisarski RD, Rischke DH. *Phys. Rev.* D61:074017 (2000)
12. Hong, DK. *Nucl. Phys.* B 582:451 (2000); Hong, DK. *Phys. Lett.* B473:118 (2000)
13. Pisarski RD, Rischke DH. *Phys. Rev.* D61:051501 (2000)

14. Hong DK, Miransky VA, Shovkovy IA, Wijewardhana LC. *Phys. Rev.* D61:056001 (2000); erratum *Phys. Rev.* D62:059903 (2000)
15. Brown WE, Liu JT, Ren H. *Phys. Rev.* D61:114012 (2000); *Phys. Rev.* D62:054016 (2000); *Phys. Rev.* D62:054013 (2000)
16. Hsu SD, Schwetz M. *Nucl. Phys.* B572:211 (2000)
17. Schäfer T. *Nucl. Phys.* B575:269 (2000)
18. Shovkovy IA, Wijewardhana LC. *Phys. Lett.* B470:189 (1999)
19. Rajagopal K, Shuster E. hep-ph/0004074 (2000)
20. Agasian N, Kerbikov B, Shevchenko, V. *Phys. Rept.* 320:131 (1999)
21. Ebert D, Klimenko K, Toki H. hep-ph/0011273
22. Berges J, Rajagopal K. *Nucl. Phys.* B538:215 (1999)
23. Carter G W, Diakonov D. *Phys. Rev.* D60:016004 (1999)
24. Iwasaki M, Iwado T. *Phys. Lett.* B350:163 (1995); Iwasaki M. *Prog. Theor. Phys. Suppl.* 120:187 (1995);
25. Alford M, Rajagopal K, Wilczek F, *Nucl. Phys.* B537:443 (1999)
26. Schäfer T, Wilczek F. *Phys. Lett.* B450:325 (1999)
27. Evans N, Hsu S, Schwetz M, hep-ph/9810514, hep-ph/9808444
28. Vanderheyden B, Jackson AD. *Phys. Rev.* D62:094010 (2000); Pepin S, Schäfer A. hep-ph/0010225 (2000)
29. Rischke D, Son D, Stephanov M. hep-ph/0011379 (2000)
30. Alford M, Bowers J, Rajagopal K, in preparation
31. Sannino F. *Phys. Lett.* B480:280 (2000)
32. Hsu S, Sannino F, Schwetz M. hep-ph/0006059 (2000)
33. Berges J. hep-ph/0012013 (2000)
34. Srednicki M, Susskind L. *Nucl. Phys.* B187:93 (1981)
35. Schäfer T, Wilczek F. *Phys. Rev. Lett.* 82:3956 (1999)
36. Evans N, Hormuzdiar J, Hsu S, Schwetz M. *Nucl. Phys.* B581:391 (2000)
37. Pisarski R, Rischke D. Proceedings of the Judah Eisenberg Memorial Symposium, 'Nuclear Matter, Hot and Cold', Tel Aviv, April 14 - 16, 1999
38. Alford M, Berges J, Rajagopal K. *Nucl. Phys.* B558:219 (1999)
39. Halasz M, Jackson A, Shrock R, Stephanov M, Verbaarschot J. *Phys. Rev.* D58:096007 (1998)
40. Berges J, Jungnickel D-U, Wetterich C. hep-ph/9811387
41. Pisarski RD, Rischke DH. *Phys. Rev. Lett.* 83:37 (1999)
42. Stephanov M. *Phys. Rev. Lett.* 76:4472 (1996)
43. Schäfer T. hep-ph/0006034 (2000)
44. Kaplan DB, Nelson AE. *Phys. Lett.* B175:57 (1986)
45. Brown G, Kubodera K, Rho M. *Phys. Lett.* B175:57 (1987)
46. Schäfer T. hep-ph/0007021 (2000)
47. Rajagopal K, Wilczek F. hep-ph/0012039 (2000)
48. Pisarski R. *Phys. Rev.* C62:035202 (2000)
49. Iwasaki M, Iwado T. *Prog. Theor. Phys.* 94:1073 (1995)
50. Rapp R, Shuryak E, Zahed I. hep-ph/0008207 (2000)
51. Clogston AM. *Phys. Rev. Lett.* 9:266 (1962); Chandrasekhar BS. *App. Phys. Lett.* 1:7 (1962)
52. Alford M, Bowers J, Rajagopal K, hep-ph/0008208 (2000)
53. Sedrakian A, Lombardo U. *Phys. Rev. Lett.* 84:602 (2000)
54. Schäfer T, Wilczek F. *Phys. Rev.* D60:074014 (1999)
55. Bedaque PF. hep-ph/9910247 (1999)
56. Larkin AI, Ovchinnikov YuN. *Zh. Eksp. Teor. Fiz.* 47:1136 (1964); translation: *Sov. Phys. JETP* 20:762 (1965)
57. Fulde P, Ferrell RA. *Phys. Rev.* 135:A550 (1964)
58. Takada S, Izuyama T. *Prog. Theor. Phys.* 41:635 (1969)
59. Heiselberg H, Pandharipande V. *Annu. Rev. Nucl. Part. Sci.* 50:481 (2000)
60. Page D, Prakash M, Lattimer JM, Steiner A. hep-ph/0005094 (2000)
61. Schaab C, et al. *Astrophys. Lett. J.* 480:L111 (1997) and references therein
62. Blaschke D, Klahn T, Voskresensky DN. *Astrophys. J.* 533:406 (2000)
63. Son D, Stephanov M. *Phys. Rev.* D61:074012 (2000); Rho M, Wirzba A, Zahed I. *Phys. Lett.* B473:126 (2000); Casalbuoni R, Gatto R. hep-ph/9911223 (1999); Hong D, Lee T, Min D. *Phys. Lett.* B477:137 (2000); Manuel C, Tytgat M. *Phys. Lett.* B479:190 (2000); Beane S,

- Bedaque P, Savage M. *Phys. Lett.* B483:131 (2000)
64. Carter G W, Reddy S. hep-ph/0005228 (2000)
 65. Madsen J. *Phys. Rev. Lett.* 85:10 (2000)
 66. Bildsten L, Ushomirsky G, astro-ph/9911155 (1999)
 67. Blaschke D, Sedrakian DM, Shahabasian KM. *Astron. Astrophys.* 350:L47 (1999)
 68. Alford M, Berges J, Rajagopal K. *Nucl. Phys.* B571:269 (2000)
 69. Sauls J. in *Timing Neutron Stars*, Öggleman J and van den Heuvel EPJ, eds., (Kluwer, Dordrecht: 1989) 457.
 70. Srinivasan G, Bhattacharya D, Muslimov AG, Tsyagan AI. *Curr. Sci.* 51:31 (1990)
 71. Bhattacharya D, Srinivasan G. *X-Ray Binaries*, Lewin WHG, van Paradijs J, van den Heuvel EPJ eds., (Cambridge University Press, 1995) 495
 72. Ruderman M. *Astrophys. J.* 366:261 (1991); *Astrophys. J.* 382:576 (1991); *Astrophys. J.* 382:587 (1991)
 73. Ruderman M, Zhu T, Chen K. *Astrophys. J.* 492:267 (1998)
 74. Hsu S. nucl-th/9903039 (1999)
 75. Lorimer D, Bailes M, Harrison P. *MNRAS* 289:592 (1997)
 76. Alpar MA, Ho C. *Mon. Not. Astron. Soc. R.* 204:655 (1983). For a recent review, see Lyne, A in *Pulsars: Problems and Progress*, Johnston S, Walker MA, Bailes M, eds., 73 (ASP, 1996)
 77. For reviews, see Pines D, Alpar A. *Nature* 316:27 (1985); Pines D, in *Neutron Stars: Theory and Observation*, Venturaand J Pines D, eds., 57 (Kluwer, 1991); Alpar MA, in *The Lives of Neutron Stars*, Alpar MA et al., eds., 185 (Kluwer, 1995). For more recent developments and references to further work, see Ruderman M, *Astrophys. J.* 382:587 (1991); Epstein RI, Baym G, *Astrophys. J.* 387:276 (1992); Alpar MA, Chau HF, Cheng KS, Pines D, *Astrophys. J.* 409:345 (1993); Link B, Epstein RI, *Astrophys. J.* 457:844 (1996); Ruderman M, Zhu T, Chen K, *Astrophys. J.* 492:267 (1998); Sedrakian A, Cordes JM, *Mon. Not. Astron. Soc. R.* 307:365 (1999)
 78. Modler R, et al. *Phys. Rev. Lett.* 76:1292 (1996)
 79. Anderson PW, Itoh N. *Nature* 256:25 (1975)
 80. Alpar MA, *Astrophys. J.* 213:527 (1977)
 81. Alpar MA, Anderson PW, Pines D, Shaham J. *Astrophys. J.* 278:791 (1984)
 82. Haensel P, Zdunik JL, Schaeffer R. *Astron. Astrophys.* 160:121 (1986)
 83. Alcock C, Farhi E, Olinto A. *Phys. Rev. Lett.* 57:2088 (1986); *Astrophys. J.* 310:261 (1986)
 84. Glendenning NK, Weber F. *Astrophys. J.* 400:647 (1992)
 85. Alpar A. *Phys. Rev. Lett.* 58:2152 (1987)
 86. Madsen J. *Phys. Rev. Lett.* 61:2909 (1988)
 87. Caldwell RR, Friedman JL. *Phys. Lett.* B264:143 (1991)
 88. Berges J, Wetterich C. hep-ph/0012311 (2000)